

MASTER

SAE-DCC evaluation and comparison with popular congestion control algorithms of V2X communication

Wei, Y.

*Award date:*  
2017

[Link to publication](#)

**Disclaimer**

This document contains a student thesis (bachelor's or master's), as authored by a student at Eindhoven University of Technology. Student theses are made available in the TU/e repository upon obtaining the required degree. The grade received is not published on the document as presented in the repository. The required complexity or quality of research of student theses may vary by program, and the required minimum study period may vary in duration.

**General rights**

Copyright and moral rights for the publications made accessible in the public portal are retained by the authors and/or other copyright owners and it is a condition of accessing publications that users recognise and abide by the legal requirements associated with these rights.

- Users may download and print one copy of any publication from the public portal for the purpose of private study or research.
- You may not further distribute the material or use it for any profit-making activity or commercial gain

**Take down policy**

If you believe that this document breaches copyright please contact us providing details, and we will remove access to the work immediately and investigate your claim.

# SAE-DCC Evaluation and Comparison with Popular Congestion Control Algorithms of V2X Communication

*Master Thesis*

Yongyi Wei

Supervisors:

Prof.dr.ir. Sonia Heemstra de Groot

Dr. Hong Li

Chetan Belagal Math

Eindhoven, Aug.31<sup>st</sup>, 2017



# Abstract

Vehicle-to-Infrastructure (V2X) communications are promising solutions to optimize the traffic efficiency and safety. However, the communication channel may get congested under a high vehicular density and furthermore degrade the reliability of safety applications if there is no congestion control mechanism introduced. In order to tackle this critical issue, various Decentralized Congestion Control (DCC) algorithms have been proposed. Each DCC adjusts different transmission parameters (message rate, data rate, transmission power, etc.) to maintain the channel load below the threshold. In this paper, we conducted a detailed study of the DCC proposed by Society of Automotive Engineers International (SAE-DCC) and then compared it with other two selected DCCs. SAE-DCC tunes the message rate w.r.t the count of vehicles within 100-meter range and adjusts the radiated power w.r.t the Channel Busy Ratio (CBR), if there are no critical events or the vehicle dynamics condition is not met. If a critical event occurs or if the vehicle dynamics condition is met, a packet will be transmitted immediately with maximum allowed radiated power. Message rate DCC is represented by LIMERIC, which is a function of CBR and guarantees a fair selection of message rate. Packet count based Data-Rate DCC (PDR-DCC), as a representative of data-rate based control algorithms, adjusts the data rate based on the count of sensed packet to enforce fairness. In our study, we firstly verified the effectiveness of SAE-DCC under different traffic densities. Secondly, we benchmarked SAE-DCC with LIMERIC and PDR-DCC using selected evaluation metrics (CBR, Inter-Reception Time (IRT), position error, T-window reliability and maximum awareness range). According to the simulation results in NS3, in terms of IRT and position error, PDR-DCC demonstrates the best performance within 200-meter range, while SAE-DCC and LIMERIC outperform PDR-DCC when the distance increases. In view of T-window reliability, PDR-DCC shows a clear advantage under dense and extreme traffic densities.

# Acknowledgement

I would like to express my sincere gratitude to Dr. Hong Li for his enlightening guidance and continuous support from the very first day. As my supervisor at NXP, Dr. Hong Li encouraged me to be my own leader in my research topic and always inspired me with his profound insights and motivation. Special thanks from the bottom of my heart go to my graduation supervisor in TU/e, Prof.dr.ir. Sonia Heemstra de Groot for her assistance throughout the whole project. I sincerely appreciate her valuable comments on my project during each progress meeting and her efforts on the composition of the assessment committee. I would also like to thank my daily supervisor Chetan Belagal Math for his help on every aspect. He was always pleased and patient to solve my problems whenever I have any doubts in literature study and implementation.

I would also extend my acknowledgment to Dr. Bas Luttik for introducing me to this amazing project. In addition, I am sincerely grateful to NXP semiconductors for the wonderful working environment with all the support I need.

I am always grateful to my family, especially my parents back in China. Whenever I have a hard time, they are always there for me. Finally, I would express my earnest gratefulness to my friends for all the encouragement and happiness they brought to me.

# Contents

Contents	iv
Abbreviations	vi
List of Figures	vii
List of Tables	viii
<b>1 Introduction</b>	<b>1</b>
1.1 Intelligent Transportation Systems	1
1.2 Vehicle-to-Everything Communication	1
1.2.1 CAM Packet and DENM Packet	1
1.2.2 BSM Packet	2
1.3 Problem Statement	2
1.4 Thesis Structure	3
<b>2 Related Work</b>	<b>4</b>
2.1 State-of-Art DCC	4
2.1.1 LIMERIC	4
2.1.2 PDR-DCC	5
2.2 Reliability Analysis for Vehicle Safety Communication Systems	6
2.2.1 Communication-level Reliability	6
2.2.2 Application-level Reliability	6
<b>3 SAE-DCC Algorithm</b>	<b>7</b>
3.1 Computational Interval	7
3.2 Important Inputs	7
3.2.1 Channel Busy Percent	7
3.2.2 Packet Error Ratio	8
3.2.3 Vehicle Density in Range	8
3.2.4 Channel Quality Indicator	8
3.3 Schedule Transmission	8
3.3.1 Basic Packet Generation	8
3.3.2 Packet Generation Based on Critical Event	9
3.3.3 Packet Generation Based on Vehicle Dynamics	9
3.4 Time Diagrams of Different Scenarios	10
3.4.1 Basic Scenario	11
3.4.2 Vehicle Dynamics Scenario	11
3.4.3 Critical Event Scenario	11

---

<b>4</b>	<b>Implementation</b>	<b>12</b>
4.1	Simulation Scenario . . . . .	12
4.2	Simulation Settings . . . . .	13
4.3	Implementation of SAE-DCC . . . . .	14
4.3.1	WAVE Protocol Stacks . . . . .	14
4.3.2	Code Design of SAE-DCC . . . . .	14
<b>5</b>	<b>Performance Evaluation</b>	<b>16</b>
5.1	Evaluation Metrics . . . . .	16
5.1.1	CBR . . . . .	16
5.1.2	IRT . . . . .	16
5.1.3	Position Error . . . . .	16
5.1.4	T-window reliability . . . . .	17
5.1.5	Maximum Awareness Range . . . . .	17
5.2	Numerical Results Discussion . . . . .	17
5.2.1	Performance of SAE-DCC . . . . .	17
5.2.2	Comparison of CBR . . . . .	18
5.2.3	Comparison of IRT . . . . .	19
5.2.4	Comparison of Position Error . . . . .	21
5.2.5	Comparison of T-window Reliability . . . . .	22
5.2.6	Comparison of Maximum Awareness Range . . . . .	23
5.2.7	Impact of CCA Busy Threshold on SAE-DCC . . . . .	24
<b>6</b>	<b>Conclusion and Future Work</b>	<b>27</b>
6.1	Conclusions . . . . .	27
6.2	Future Work . . . . .	27
	<b>Bibliography</b>	<b>29</b>

# Abbreviations

<b>CAM</b>	Cooperative Awareness Message
<b>CBP</b>	Channel Busy Percent
<b>CBR</b>	Channel Busy Ratio
<b>CCA</b>	Clear Channel Assessment
<b>DCC</b>	Decentralized Congestion Control
<b>DENM</b>	Decentralized Environmental Notification Message
<b>ERF</b>	Effective Risk Factor
<b>ESTI</b>	European Telecommunication Standards Institute
<b>HV</b>	Host Vehicle
<b>IRT</b>	Inter-Reception Time
<b>ITS</b>	Intelligent Transportation System
<b>LIMERIC</b>	Linear MESSage Rate Integrated Control
<b>MAX-ITT</b>	Max Inter-Transmit Time
<b>PDR</b>	Packet Delivery Ratio
<b>PDR-DCC</b>	Packet count based Data-Rate Decentralized Congestion Control
<b>PER</b>	Packet Error Ratio
<b>RV</b>	Remote Vehicle
<b>SAE-DCC</b>	Society of Automotive Engineers proposed Decentralized Congestion Control
<b>SUMO</b>	Simulation of Urban MObility
<b>V2I</b>	Vehicle-to-Infrastructure
<b>V2V</b>	Vehicle-to-Vehicle
<b>V2X</b>	Vehicle-to-Everything
<b>VANET</b>	Vehicular Ad-hoc NETwork
<b>WAVE</b>	Wireless Access in Vehicular Environments

# List of Figures

3.1	Sliding window for calculating PER . . . . .	8
3.2	2D Position Extrapolation . . . . .	10
3.3	Time diagram of BSM generation without events or vehicle dynamics . . . . .	11
3.4	Time diagram of BSM generation when vehicle dynamics condition is met . . . . .	11
3.5	Time diagram of BSM generation when a critical event occurs . . . . .	11
4.1	The highway scenario simulated in SUMO . . . . .	12
4.2	SAE-DCC implementation flow chart . . . . .	14
5.1	CBR in the observing zone of SAE-DCC vs Time for different vehicular densities . . . . .	18
5.2	CBR vs Time for different vehicular densities . . . . .	19
5.3	95% IRT vs distance in medium scenario . . . . .	20
5.4	95% IRT vs distance in dense scenario . . . . .	20
5.5	95% IRT vs distance in extreme scenario . . . . .	21
5.6	95% position error vs distance in medium scenario . . . . .	21
5.7	95% position error vs distance in dense scenario . . . . .	22
5.8	95% position error vs distance in extreme scenario . . . . .	22
5.9	T-window reliability (N=1, T=1) under different traffic densities . . . . .	23
5.10	T-window reliability (N=2, T=1) under different traffic densities . . . . .	23
5.11	CBR comparison of SAE-DCC with different CCA busy thresholds in medium scenario . . . . .	24
5.12	95% IRT comparison of SAE-DCC with different CCA busy thresholds in medium scenario . . . . .	25
5.13	95% Position error comparison of SAE-DCC with different CCA busy thresholds in medium scenario . . . . .	25
5.14	T-window reliability (N=1, T=1) comparison of SAE-DCC with different CCA busy thresholds in medium density scenario . . . . .	26



# List of Tables

4.1	The traffic densities and mobility parameters in various scenarios . . . . .	13
4.2	Simulation parameters . . . . .	13
4.3	Algorithm parameters . . . . .	14
5.1	Average message rate of SAE-DCC in different scenarios . . . . .	18
5.2	Average radiated power of SAE-DCC in different scenarios . . . . .	18
5.3	Average CBR and standard variance in stable phase of three DCCs . . . . .	19
5.4	Maximum awareness range for different application requirements under various traffic densities . . . . .	24

# Chapter 1

## Introduction

### 1.1 Intelligent Transportation Systems

Due to the increasing number of vehicles, traffic accidents and traffic congestion have become a world-wide problem. According to the data released by National Safety Council, in 2015, 38,300 people were killed on US road as well as 4.4 million people were reported injured in traffic accidents. The number of death rose by 8 percent from 2014, which has been the highest jump ever. In addition, traffic congestion led to a economic cost of 160 billion dollars in the US in 2014 and this number is estimated to reach 192 billion dollars by 2020 [1].

Intelligent Transportation Systems (ITS) are promising solutions to improve traffic safety and efficiency through integrating communication technologies into vehicles and transportation infrastructures to create a comprehensive real-time transportation management system in a wide area. Vehicular Ad-hoc NETWORKS (VANETs), where both Vehicle-to-Vehicle (V2V) and Vehicle-to-Infrastructure (V2I) communications co-exist, are key components in ITS framework to improve traffic safety and efficiency.

### 1.2 Vehicle-to-Everything Communication

VANETs support various safety applications for different safety aspects, for instance the Emergency Electronic Brake Lights and the Forward Crash Warning. Aiming at optimizing the traffic safety and efficiency, these safety applications rely on beacon messages broadcast by each vehicle to its neighbor vehicles and roadside units.

A technology implemented in Vehicle-to-Everything (V2X) communications is Dedicated Short Range Communications (DSRC). IEEE 802.11p is selected as the MAC layer and Physical layer of the DSRC. The US Federal Communication Commissions have allocated 75 MHz of spectrum in 5.9 GHz range for DSRC to be used by ITS [2].

#### 1.2.1 CAM Packet and DENM Packet

In Europe, European Telecommunications Standards Institute (ETSI) has specified the Cooperative Awareness Basic Service, which provides safety information by exchanging periodic and event-driven message packets between vehicles. To support this service, ETSI has defined two kinds of messages, CAM packets and DENM packets.

A CAM packet includes information of vehicle position, heading, velocity, and other basic attributes. CAM packets are periodically broadcast to neighbor vehicles and roadside units within a single hop distance. The majority of safety applications are benefiting from CAMs. The message generation rate of CAM ranges from 1 Hz to 10 Hz. When congestion control condition is not met, CAMs are generated according to vehicle dynamics. Generation rules are checked every 100 ms and a CAM will be generated if one of the following conditions is met: (i) the heading difference

is larger than 4 degrees; (ii) the distance difference is larger than 5 m; (iii) the absolute velocity difference is larger than 1 m/s.

DENMs are event-driven. These messages will be generated and broadcast to neighbor vehicles only if critical events occur. DENMs are designed for the Cooperative Road Hazard Warning to warn neighbor nodes about detected hazards. The triggering conditions and termination conditions of DENM messages corresponding to various events have been properly defined in [3].

### 1.2.2 BSM Packet

In the US, the beacon messages used by safety applications in V2X communication are called Basic Safety Messages (BSM) as defined in [4]. A BSM consists of two parts. Part I is the mandatory part for a valid BSM packet, including the essential state information (vehicle velocity, heading, packet time stamp, message count, longitude, latitude, brake system status, etc). Part II is optional and is included in the BSM packet only if it is necessary depending on event condition.

If no critical event occurs, the BSM packet generation is periodic or is based on the congestion control algorithm. However, if a critical event condition is met, a BSM packet with EventFlag in BSM Part II needs to be generated immediately.

## 1.3 Problem Statement

On-board V2V communication systems are designed for vehicles to exchange their basic information with neighbor vehicles, in order to optimize the safety and the effectiveness of transportation. However, with an increasing density of vehicles in the network, the communication channel gets busier, which may lead to the channel congestion. A congested channel can lead to a higher probability of packet collision, causing packet loss and then degrading the safety application reliability. Therefore, various congestion control approaches have been created to mitigate this problem by tuning the transmission behavior according to the channel load in order to effectively maintain the reliability of safety applications.

Generally, congestion control approaches can be either centralized or decentralized. In the centralized congestion control approach, a central entity decides the operational parameters of all the vehicles in a certain area. One significant disadvantage of the centralized congestion control is the high requirement of extremely large computation on the central entity, which makes it unrealistic to be implemented in real traffic network. In the distributed or decentralized approaches, each vehicle in the network performs the congestion control algorithm independently[5]. Because of the high mobility and uncertainty of each individual vehicle, decentralized approaches are preferred for congestion control. Thus, we only discuss the Decentralized Congestion Controls (DCC) in this thesis.

One prominent DCC approach is to adjust the number of transmission packets per unit time to reach the goal of congestion control. This algorithm uses the Channel Busy Ratio (CBR) as input to adjust the message rate and converge the channel utilization to a desired target level. Linear Message Rate Integrated Control (LIMERIC), proposed by authors in [6], is a typical representative of message-rate DCC algorithms. Another popular DCC approach is to adjust the data rate. When the communication channel gets busy, each vehicle in the network increases its data rate so that packets are transmitted in a shorter air time. Packet Count Based Decentralized Data-Rate Congestion Control (PDR-DCC) proposed by authors in [7] represents the data-rate based DCC approaches. This algorithm uses the packet count as an input to maintain the channel utilization under threshold value.

Society of Automotive Engineers (SAE) also specified a solution to congestion control in [8]. In order to manage congestion control, the SAE Decentralized Congestion Control (SAE-DCC) adjusts the message rate and the transmission power in response to the vehicle count within 100-meter range and the CBR respectively. As having been explained before, reducing the message rate can decrease the number of transmitted packets in a given time period. Meanwhile, reducing the transmission power can shorten the transmission range such that fewer vehicles would sense the

transmitted message packet. Both two approaches combined in SAE-DCC lead to a less congested channel.

Each DCC has its own advantages and disadvantages. One metric for evaluating the performance of DCC is its ability of converging the channel utilization to the target threshold in different density scenarios. In addition, while maintaining the channel utilization below threshold, DCCs may also degrade the reliability of safety applications. In terms of the message rate and the communication range, safety applications have different communication requirements. Most of the periodic message packets require a message rate ranging from 1 Hz to 10 Hz while event-given packets generally require a higher message rate. Meanwhile, most safety applications have a requirement for communication range between 50 m and 300 m. For example, the traffic signal violation warning requires a message rate of 10 Hz and a maximum communication range of 250 m, while the curve speed warning application requires a message rate of only 1 Hz and a maximum communication range of 200 m [9]. However, two possible outcomes after introducing DCCs to the vehicle communication network are lowering the message rate and shortening the communication range, which may violate the safety application requirement. Therefore, except for the ability of converging the channel utilization to the target threshold, the impact on the reliability of safety applications caused by DCCs should also be considered.

The main contributions of this paper are twofold:

1. We conduct this study to analyze and evaluate the effectiveness of SAE-DCC under different vehicular densities.
2. We benchmark SAE-DCC with other two DCCs in three scenarios with various traffic densities to understand its strengths and weaknesses. The other two selected DCC algorithms are LIMERIC and PDR-DCC. Through simulation via NS3 simulator under various traffic densities, We have analyzed and assessed the performance of three DCC algorithms using selected evaluation metrics. The chosen metrics are channel busy ratio, position error, inter-reception time, T-Window reliability and maximum awareness range.

## 1.4 Thesis Structure

The rest of this thesis is structured as follows: In Chapter 2, we present the related work and state-of-art DCCs. A detailed description of SAE-DCC algorithm is explained in Chapter 3. In Chapter 4, we introduce the implementation details, including simulation tools and settings. The selected evaluation metrics and numeric results are presented in Chapter 5. In Chapter 6, we conclude our study and give suggestions on further research topics.

# Chapter 2

## Related Work

### 2.1 State-of-Art DCC

Various researches related to DCC have been conducted in order to tackle congested communication channels. Among all DCC algorithms, a majority of them adopt CBR as the measurement of channel utilization. DCC algorithms can be categorized based on which transmission parameter is adjusted.

Message rate control algorithms adjust the message rate to control the number of transmitted packet per unit time to reach the goal of congestion control. AIMD proposed by authors in [10] and LIMERIC proposed by authors in [6] are the two most discussed message rate control algorithms. Inspired by LIMERIC, authors in [11] proposed EMBARC, which is extended from LIMERIC. EMBARC allows the system to schedule a packet transmission according to the vehicular movement. This algorithm guarantees a higher transmission probability for vehicles with higher dynamics in order to reduce the tracking error. In general, lowering the message rate can effectively control the channel loads below a threshold. However, in some extreme scenarios with a high vehicular density, the message rate can be tuned to a significantly low value, which would have negative impacts on the reliability of some safety applications.

Transmission power adaption algorithms tune the transmission power to narrow the broadcast range in order to obtain the target of congestion control. The power control algorithm proposed by authors in [12] is a typical representative. This algorithm adjusts the transmission power such that the number of neighbor vehicles of a certain vehicle always stays within a minimum and maximum threshold. Yet for very dense scenario, it would lead to a very short awareness distance, which might be insufficient for the safety requirement.

Data rate based control algorithms reduce the air time of each packet by controlling the data rate to maintain the channel busy ratio below the threshold value. Date Rate-DCC(DR-DCC) proposed by authors in [5] and PDR-DCC proposed by authors in [7] are two typical representatives. Based on IEEE 802.11p standard, allowed data rates are from 3 Mbps to 27 Mbps. However, a lower value of data rate is preferred and most DCC algorithms select 6 Mbps, as a higher data rate has to compromise its robustness against interferences and noises [13].

In addition to the DCCs that adjust only one transmission parameter, some researches on algorithms combining the transmission power adaption with the message rate adaption have also been conducted. For example, authors in [14] proposed a joint power/rate DCC that selects transmission power with respect to the target communication distance and tunes message rate with respect to the channel utilization. However, one challenge of joint DCCs is to find the optimal match of the message rate and the transmission power.

#### 2.1.1 LIMERIC

LIMERIC is a DCC that targets at converging the channel load to a desired threshold by controlling the message rate based on CBR. In addition to maintaining a desired channel utilization, LIMERIC

also ensures a fair message rate among neighbor vehicles.

There are two essential inputs for LIMERIC,  $CBR_T$  and  $CBR_k(t)$ .  $CBR_T$  is the target channel load that the system intends to reach.  $CBR_k(t)$ , calculated by vehicle  $k$ , is the global channel busy ratio created by all the vehicles within its interference area. With the above information, vehicle  $k$  is able to adjust its message rate  $R_k(t)$  as presented in Equation 2.1:

$$R_k(t) = (1 - \alpha) \times R_k(t - T) + \beta \times (CBR_T - CBR_k(t - T)) \quad (2.1)$$

Where  $T$  is the CBR measurement period (in this thesis  $T$  is set to 200 ms),  $\alpha$  and  $\beta$  are adaption parameters influencing the steady state convergence and stability.  $\beta$  plays a considerably important role on the ability of ensuring convergent behavior while the impact of  $\alpha$  is more related to the equilibrium and the speed of convergence. A good trade-off should be considered while determining the values of these two parameters. A more detailed discussion on the selection of adaption parameters can be found in [6].

After the initial phase, LIMERIC manages to converge CBR to  $CBR_{con}$  while guaranteeing a fair message rate for all vehicles, as proven in Equation 2.2:

$$CBR_{con} = \frac{n \times \beta}{\alpha + n \times \beta} \times CBR_T \quad (2.2)$$

where  $n$  denotes the count of cars in the communication area.

### 2.1.2 PDR-DCC

PDR-DCC, as a representative of data-rate based DCC, adjusts the data rate according to CBR in combination with the packet count  $P_C$ . It ensures a fair selection of data rates.

PDR-DCC is described in Algorithm 1.  $P_C$ , denoting the number of packets in the channel sensed by a vehicle within a measurement interval  $\theta$ , is a decisive input to PDR-DCC. A detailed description of packet count estimation can be found in [7].

---

**Algorithm 1** PDR-DCC algorithm [7]

---

```

1: while PDR-DCC active do
2: get  $P_C$  periodically for  $\theta$  seconds
3:   if  $P_C < \frac{CBR_T \times \theta}{T_3}$  then
4:      $D = 3Mbps$ 
5:   else if  $P_C > \frac{CBR_T \times \theta}{T_3}$  and  $P_C < \frac{CBR_T \times \theta}{T_6}$  then
6:      $D = 6Mbps$ 
7:   else if  $P_C > \frac{CBR_T \times \theta}{T_6}$  and  $P_C < \frac{CBR_T \times \theta}{T_9}$  then
8:      $D = 9Mbps$ 
9:   else if  $P_C > \frac{CBR_T \times \theta}{T_9}$  and  $P_C < \frac{CBR_T \times \theta}{T_{12}}$  then
10:     $D = 12Mbps$ 
11:  else if  $P_C > \frac{CBR_T \times \theta}{T_{12}}$  and  $P_C < \frac{CBR_T \times \theta}{T_{18}}$  then
12:     $D = 18Mbps$ 
13:  else
14:     $D = 24Mbps$ 
15:  end if
16: end while

```

---

As shown in Algorithm 1,  $P_C$  is computed every  $\theta$  seconds (in this thesis  $\theta$  is set to 100 ms). The values of  $P_C$  are categorized into 6 levels and each level corresponds to a different data rate. The selected data rate  $D$  manages to converge the CBR to  $CBR_T$ .  $T_D$  denotes the required transmission time of a packet for different data rates, where  $D$  indicates the various data rates from 3 Mbps to 24 Mbps. Each vehicle independently chooses the minimum possible data rate to avoid congestion and also to obtain a maximum possible communication range.

## 2.2 Reliability Analysis for Vehicle Safety Communication Systems

As explained above, the introduction of DCCs to Vehicle Safety Communication may violate the safety application requirement. Thus, the reliability analysis of DSRC for vehicle safety applications is also critical to the performance of DCC algorithms. Several researches related to the reliability analysis in VANET have been conducted.

Authors in [15] proposed two levels of reliability, the communication-level reliability and the safety application-level reliability. The communication reliability focuses on the link-level behavior between a pair of nodes. Generally, the percentage of successfully delivered packets is an important indication of communication-level reliability and it varies in different traffic scenarios due to the different channel quality. However, the application-level reliability is more end user oriented. Even though there are some packets that cannot be delivered successfully sometimes, the end users would not experience undesired outcome given the fact that some applications require only a certain number of successfully delivered packets within one second.

### 2.2.1 Communication-level Reliability

The most widely used communication-level reliability metric is Packet Delivery Ratio (PDR), denoting the probability of successfully delivering a packet to the Remote Vehicle (RV) from the Host Vehicle (HV). One most used approach to calculate PDR is to compute the ratio of the received packet count and the total number of expected packets within a predefined period.

As PDR is an average estimation of the communication-level reliability, it may omit the hazards caused by adjacent packet loss. Thus, authors in [15] proposed another metric, distribution of consecutive packet drops. It aims at detecting the potential danger caused by consecutive packet drops which is not illustrated by PDR.

Authors in [16] proposed a metric that indicates the freshness of the received packet, packet Inter-Reception Time (IRT). It is specified as the time difference in seconds or milliseconds between time instances of two adjacent received packets from the same HV.

### 2.2.2 Application-level Reliability

One prominent metric for assessing the safety application reliability is T-window reliability. It is defined as the probability of successfully receiving at least N packet from neighbor vehicles during a tolerance time window T [15]. As explained previously, each safety application requires receiving different numbers of packets within a certain period. T-window reliability can be adopted to evaluate the reliability for individual safety application by adjusting the value of N and T.

Authors in [17] proposed a novel metric called Effective Risk Factor (ERF). This metric is extended from T-window reliability but takes also the distance between a pair of nodes in to consideration to quantify the application risk, because a close-by neighbor vehicle's invisibility is more risky than a far-off vehicle's loss of visibility. Thus, the calculation of ERF is based on the number of consecutive T-window reliability failures and the distance between a pair of vehicles to quantify the risk that each individual vehicle takes.

Authors in [18] proposed a metric called position error. It is specified as the distance in meters between the HV's real position and the RV's speculation of the HV's position. Position error is related to IRT but it is a more application-oriented metric, as it indicates the accuracy of the receiver's tracking of the transmitter's movement.

## Chapter 3

# SAE-DCC Algorithm

This chapter describes the SAE-DCC algorithm.

SAE-DCC takes multiple transmission parameters into consideration to address the channel congestion issue. The system adjusts the message rate according to the vehicle density and adjusts the radiated power with respect to the channel loads. Besides, the system generates BSM immediately and transmits it with maximum radiated power whenever a critical event occurs or the vehicle dynamics condition is met. A detailed description of this algorithm will be explained in the following sections.

### 3.1 Computational Interval

Firstly, the computational intervals used in the SAE-DCC algorithm need to be clarified. These intervals are channel busy percent measurement interval  $vCBPMeasInt$  (100 ms), packet error ratio subinterval  $vPERSubInterval$  (1 s), packet error ratio interval  $vPERInterval$  (5 s), and transmission rate control interval  $vTxRateCntrlInt$  (100 ms).

### 3.2 Important Inputs

This section defines the important inputs that are used in SAE-DCC algorithm.

#### 3.2.1 Channel Busy Percent

SAE-DCC uses Channel Busy Percent (CBP) as a measure of the channel utilization. As Shown in Equation 3.1,  $RawCBP$  is calculated as the ratio of duration of the channel indicated as busy over a measurement interval  $vCBPMeasInt$ . A channel is indicated as busy if one of the following conditions is met: (i) the DSRC system is transmitting packets or (ii) Clear Channel Assessment (CCA) determines the channel is busy. As defined in 802.11 [19], CCA consists of Energy Detection and Carrier Sensing, both of which can contribute to the channel busy time.

$$RawCBP(k) = \frac{100 \times DurationChannelIndicatedasBusy}{vCBPMeasInt} \quad (3.1)$$

In order to filter the measurement noise, the system also calculate smooth CBP, as shown in Equation 3.2, introducing  $vCBPWeightFactor$  equal to 0.5.  $RawCBP$  and Smooth CBP are calculated every 100 milliseconds and Smooth CBP will be further used as an input to determine the radiated power.

$$CBP(k) = vCBPWeightFactor \times RawCBP(k) + (1 - vCBPWeightFactor) \times CBP(k-1) \quad (3.2)$$



### 3.2.2 Packet Error Ratio

Packet Error Ratio (PER) is computed between a pair of HV and RV using a sliding window with a `vPERInterval` (5s) and a `vPERSubInterval` (1s) as shown in Figure 3.1. As we can see in the figure, the length of  $\delta_k$  is 5 times the length of  $w_k$ .

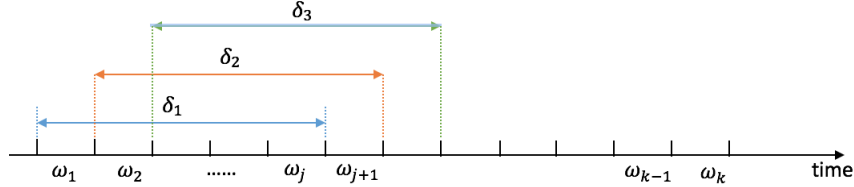


Figure 3.1: Sliding window for calculating PER

PER is computed every 1 s, as the number of missed packets divided by the number of total expected packets during the past 5 s, as shown in Equation 3.3. It will be used to calculate the channel quality indicator.

$$PER_i(k) = \frac{\text{number of missed BSMs from } RV_i \text{ during}[w_k - 4, w_k]}{\text{total expected BSMs from } RV_i \text{ during}[w_k - 4, w_k]} \quad (3.3)$$

Each HV keeps track of `DE_MsgCount` included in each BSM to determine the number of total expected BSM packets as well as the number of missed BSM packets. The total expected number of BSM packets within the 5-second sliding window is calculated as the difference between `De_MsgCount` in the first and last received BSM packets plus 1. The number of missed BSM packets is computed as the difference between actual number of received BSM packets from a certain RV and the number of total expected BSM packets.

### 3.2.3 Vehicle Density in Range

Vehicle Density in Range ( $N$ ) indicates the number of unique neighbor vehicles within the `vPER-Range` (100 m) during the past 1 s. The system checks the `DE_TemporaryID` included in BSM to decide if a certain RV is unique.  $N(k)$  is calculated every 1 s and will be further used as an input to calculate inter transmission time between BSM packets.

### 3.2.4 Channel Quality Indicator

Channel Quality Indicator ( $\Pi$ ) is calculated as the average of the PERs of all the vehicles within the `VPERRange` during the past 5 s. The system calculates  $\Pi(k)$  every 1 s at the end of the  $k^{\text{th}}$  instance of `vPERSubInterval`. If the value  $\Pi(k)$  is greater than 0.3, it will be set to 0.3. The Channel Quality Indicator will be used as an input for determining the vehicle dynamics.

## 3.3 Schedule Transmission

Having understood the important inputs for SAE-DCC, we can start to study the scheduling mechanism.

### 3.3.1 Basic Packet Generation

If no critical events occur or the vehicle dynamics condition is not met, the packet transmission is scheduled based on the Maximum Inter-Transmit Time (`MAX_ITT`). Before the calculation of `MAX_ITT`, the system firstly computes the smoothed vehicle density in range,  $N_s(k)$ , as presented

in Equation 3.4, in order to obtain a more stable value of Max\_ITT. The weight factor,  $\lambda$  (0.05), is introduced to calculate  $N_s(k)$ .

$$N_s(k) = \lambda \times N(k) + (1 - \lambda) \times N_s(k - 1) \quad (3.4)$$

Having calculated the  $N_s(k)$  at  $k^{th}$  instance, Max\_ITT(k), in milliseconds, is determined as shown in Equation 3.5. B is the density coefficient (25) and vMax\_ITT is the maximum threshold (600 ms). As derived from the Equation 3.5, the maximum message rate of SAE-DCC can reach 10 Hz while the minimum message rate is 1.67 Hz.

$$Max\_ITT(k) = \begin{cases} 100 & N_s(k) \leq B \\ 100 \times \frac{N_s(k)}{B} & B < N_s(k) < \frac{vMax\_ITT}{100} \times B \\ vMax\_ITT & \frac{vMax\_ITT}{100} \times B \leq N_s(k) \end{cases} \quad (3.5)$$

Max\_ITT is calculated every 100 ms. Each vehicle generates the next BSM packet at the interval of the most recently calculated Max\_ITT. The rationale of Equation 3.5 is to lower the message generation rate for vehicles with more neighboring vehicles, in order to reduce the packet collision.

However, the changes in the value of calculated Max\_ITT may also affect the scheduled packet generation. Having calculated a new Max\_ITT(k), the system will make decision as follows:

- If (NextScheduledMsgTime - (LastTxTime + Max\_ITT(k)))  $\geq$  vReScheduleTh (25ms)
- Then the system will cancel the scheduled packet generation and schedule the next packet generation at max (CurrentTime, LastTxTime + Max\_ITT(k)).

Before the transmission of each newly-generated BSM packet, the radiated power needs to be calculated with respect to the smoothed CBP, as presented in Equation 3.6.

$$f(CBP) = \begin{cases} vRPMax & CBP \leq vMinChanUtil \\ vRPMax - \left( \frac{vRPMax - vRPMin}{vMaxChanUtil - vMinChanUtil} \right) \times (CBP - vMinChanUtil) & vMinChanUtil < CBP < vMaxChanUtil \\ vRPMin & vMaxChanUtil \leq CBP \end{cases} \quad (3.6)$$

As denoted in Equation 3.6, when the CBP is lower than the vMinChanUtil (50%), the radiated power will reach the maximum value vRPMax (20 dBm). If the CBP is beyond vMaxChanUtil (80%), the radiated power will be set to the minimum value vRPMin (10 dBm).

In order to avoid a sudden jump for the value of the radiated power, the system calculates Base\_RP based on the previous radiated power Previous\_RP, as shown in Equation 3.7.

$$Base\_RP = Previous\_RP + vSUPRAGain \times (f(CBP) - Previous\_RP) \quad (3.7)$$

where vSUPRAGain is the Stateful Utilization-based Power Adaption Gain, which is equal to 0.5.

The rationale of tuning the radiated power is to lower the radiated power in scenarios with a high traffic density such that the communication range is shortened.

### 3.3.2 Packet Generation Based on Critical Event

If a critical event occurs, for example one or more airbags have been deployed, the system will cancel the previously scheduled BSM generation and will generate and transmit a BSM with EventFlag immediately with the maximum allowed radiated power. A list of critical events defined by SAE standard can be found in [4].

### 3.3.3 Packet Generation Based on Vehicle Dynamics

The packet generation based on vehicle dynamics is relatively complicated and it is triggered by tracking error  $e(k)$ . Tracking error is defined as the difference in distance between where a certain HV reckons its current position is and where the HV thinks the RVs estimate the HV is located at current time. The calculation can be completed following three steps every 100 ms.

1. Each HV extrapolates its current position based on its latest known status information, defined as HV Local Estimator, using the 2-D position extrapolation model with a constant speed and heading, as presented in Figure 3.2.
2. After each BSM generation, the system uses a uniform distribution function to generate a random number within the range from 0 to 1 and makes comparison of this random number and  $\prod(k)$ . If  $\text{random} \geq \prod(k)$ , it indicates that the HV reckons this BSM has been received by RVs and assumes that all the RVs have the latest status information of this HV. If  $\text{random} < \prod(k)$ , this indicates a failure of transmission, thus the RV assumes that all the RVs will not update with its latest status information. However, if there are more than three consecutive failures of transmission, the HV will assume that the latest BSM packet is successfully delivered to all the RVs and all the RVs are updated with the most recent status information of the HV. Based on the status information assumed received by the RVs, the HV computes the current position where the RVs believe the HV is located, defined as the HV Remote Estimator. The HV Remote Estimator also follows the same mechanism of the position extrapolation as presented in Figure 3.2.
3. The system calculate  $e(k)$  as the 2-D distance difference between the HV Local Estimator and the HV Estimator [8], which will be used to determine the transmission probability.

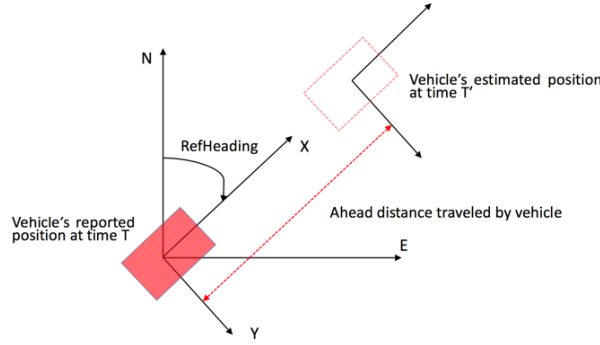


Figure 3.2: 2D Position Extrapolation

The next step is to determine the transmission possibility according to the tracking error  $e(k)$ . If  $e(k)$  is greater than the 0.5 m, the system will directly set the transmission probability as 1. If  $e(k)$  is smaller than 0.2 m, the transmission probability will be set to 0. Otherwise, the probability is within the range of 0 and 1, as presented in Equation 3.8.

$$p(k) = \begin{cases} 1 - \exp(-75 \times |e(k) - 0.2|^2) & \text{if } 0.2 \leq e(k) < 0.5 \\ 1 & \text{if } e(k) \geq 0.5 \\ 0 & \text{otherwise} \end{cases} \quad (3.8)$$

The system checks whether the vehicle dynamics condition is met every 100 ms by comparing a drawn random number between 0 and 1 with the calculated transmission probability. If the random value is not greater than the probability as well as the time difference between current time and the time when next packet is scheduled is greater than 25 ms, the vehicle dynamics condition is met. In this case, the system will cancel the previously scheduled BSM generation and will generate and transmit a BSM immediately with the maximum allowed radiated power.

### 3.4 Time Diagrams of Different Scenarios

Given the fact that SAE-DCC has a relatively complicated packet scheduling mechanism, some use cases with time diagrams are presented in this section for a better understanding about how SAE-DCC schedules the BSM generation.

### 3.4.1 Basic Scenario

Figure 3.3 illustrates the time diagram of the BSM packet generation when the critical event or vehicle dynamics condition is not met. The system calculates the Max\_ITT every 0.1 s and schedules the next BSM generation using the most recently calculated Max\_ITT. Assuming at 3.1 s, the system calculates the Max\_ITT as 0.13 s. After the generation of  $BSM_N$  at 3.13 s, the system schedules  $BSM_{N+1}$  at 3.13 s + 0.13 s = 3.26 s. Later on at 3.2 s, the system calculates Max\_ITT as 0.12 s. After the generation of  $BSM_{N+1}$  at 3.26 s as scheduled, the system schedules the generation of  $BSM_{N+2}$  at 3.26 s + 0.12 s = 3.38 s.

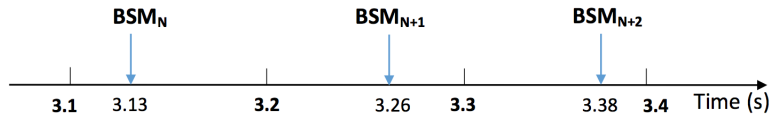


Figure 3.3: Time diagram of BSM generation without events or vehicle dynamics

### 3.4.2 Vehicle Dynamics Scenario

Figure 3.3 shows the time diagram of BSM packet generation when the vehicle dynamics condition is met. The system calculates the Max\_ITT and checks the vehicle dynamics condition every 0.1 s. Assuming at 3.1 s, the system calculates the Max\_ITT as 0.13 s. After the generation of  $BSM_N$  at 3.13 s, the system schedules  $BSM_{N+1}$  at 3.13 s + 0.13 s = 3.26 s. However, at 3.2 s, the system detects that the vehicle dynamics condition is met, hence it cancels the scheduled  $BSM_{N+1}$  and generates a BSM immediately at 3.2 s. After the generation of  $BSM_{Dynamics}$ , using the Max\_ITT (0.12 s) calculated at 3.2 s, the system schedules the generation of  $BSM_{N+2}$  at 3.2 s + 0.12 s = 3.32 s.

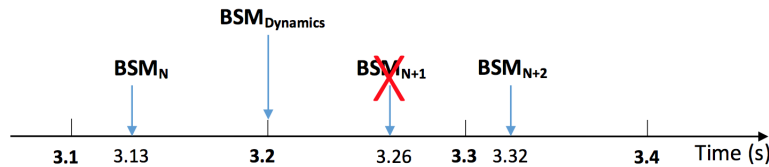


Figure 3.4: Time diagram of BSM generation when vehicle dynamics condition is met

### 3.4.3 Critical Event Scenario

Figure 3.3 demonstrates the time diagram of BSM packet generation when a critical event occurs. Assuming at 3.1 s, the system calculates the Max\_ITT as 0.13 s. After the generation of  $BSM_N$  at 3.13 s, the system schedules  $BSM_{N+1}$  at 3.13 s + 0.13 s = 3.26 s. However, a critical event occurs at 3.21s, thus the system cancels the scheduled  $BSM_{N+1}$  and generates a BSM with event flag immediately at 3.21 s. After the generation of  $BSM_{EVENT}$ , using the Max\_ITT (0.12 s) calculated at 3.2 s, the system schedules the generation of  $BSM_{N+2}$  at 3.21 s + 0.12 s = 3.33 s.

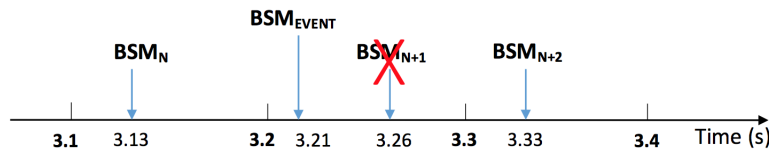


Figure 3.5: Time diagram of BSM generation when a critical event occurs

## Chapter 4

# Implementation

### 4.1 Simulation Scenario

In order to benchmark the performance of SAE-DCC, PDR-DCC and LIMERIC, we conducted a series of simulations using NS3 network simulator together with SUMO traffic simulation suite.

SUMO is an open source simulator that manages to simulate the realistic traffic systems including roadside infrastructures and vehicles with mobility. In our simulation, we adopted SUMO to create a realistic 3-kilometer highway scenario, as shown in Figure 4.1. The highway is equipped with 4 lanes in each direction and each lane is 3.3 meters wide. In this highway scenario, all the vehicles are running in a loop. Whenever a vehicle arrives at the end of the lane, it turns into the opposite direction. Considering that the traffic density might have an impact on the performance of each DCC algorithm, we built up three scenarios with various vehicular densities: 200 vehicles/km (medium), 300 vehicles/km (dense), 400 vehicles/km (extreme). The maximum allowed velocities, accelerations and decelerations for each scenario are illustrated in Table 4.1.

The vehicular mobility simulated in SUMO is generated as a trace file and it can be used in NS3 network simulator as the mobility model. For the analysis of simulation results, we only considered the vehicles in the observing zone within the range between 1 km and 2 km, as the highlighted region in Figure 4.1.

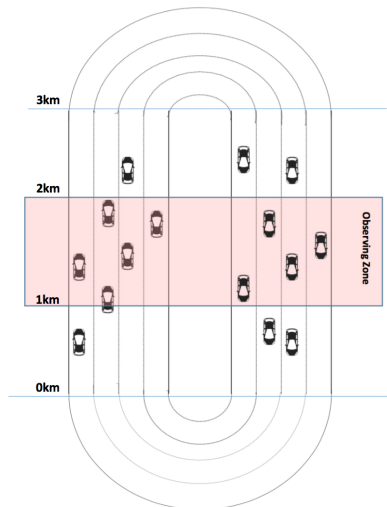


Figure 4.1: The highway scenario simulated in SUMO

Table 4.1: The traffic densities and mobility parameters in various scenarios

Scenario	Vehicular Density	Max Velocity	Max Acceleration	Max Deceleration
Medium	600cars/3km	40m/s	$1.75\text{m}/\text{s}^2$	$5\text{m}/\text{s}^2$
Dense	900cars/3km	35m/s	$1.75\text{m}/\text{s}^2$	$5\text{m}/\text{s}^2$
Extreme	1200cars/3km	24m/s	$1.75\text{m}/\text{s}^2$	$5\text{m}/\text{s}^2$

## 4.2 Simulation Settings

All the simulations are performed in NS3. We set the target channel load  $CBR_T$  as 0.7.

The simulation parameters selected for each DCC are shown in Table 4.2. Since LIMERIC and PDR-DCC are designed according to the European standard, their simulation parameters are selected as specified in [20]. SAE-DCC is an algorithm proposed by the US, hence its simulation parameters are in line with [8].

Table 4.2: Simulation parameters

CCA busy threshold	PDR-DCC: -85 dBm
	LIMERIC: -85 dBm
	SAE-DCC: -95 dBm
Received power sensitivity	PDR-DCC: -82 dBm
	LIMERIC: -82 dBm
	SAE-DCC: -92 dBm
Transmission power	PDR-DCC: 24 dBm
	LIMERIC: 24 dBm
	SAE-DCC: 10 dBm to 20 dBm
Transmission rate	PDR-RCC: 3 Mbs to 24 Mbs
	LIMERIC: 6 Mbs
	SAE-DCC: 6 Mbs
Payload size	300 bytes
Message rate	PDR-DCC: 10 Hz
	LIMERIC: Varies
	SAE-DCC: Varies
Simulation period	30 sec
Mobility	SUMO

For the propagation models, we implement dual slope path loss model in combination with Nakagami- $m$  fading model. The dual slope model is a log distance path loss model with two distance regions. In our simulation, we set the distance breakpoint as 80 m. The path loss component is 1.9 within 80 m while the path loss component increases to 3.8 when the distance is beyond 80 m. In addition to the large scale fading model, we added also Nakagami- $m$  as a small scale fading model that addresses the oscillation in the signal power due to multiple path fading. For Nakagami- $m$  model, there exist three distance ranges. From 0 m to 50 m, the fading depth parameter  $m$  is set to 3. From 51 to 150 m,  $m$  is set to 1.5. If the distance is longer than 150 m,  $m$  is set to 1.

Having set up the simulation scenario and selected proper path loss models, we also need to set the algorithm parameters for each DCC. For SAE-DCC, all the algorithm parameters are set in line with the specifications in Chapter 3. The algorithm parameters of PDR-DCC and LIMERIC are listed in Table 4.3, as discussed in [7] and [6].

Table 4.3: Algorithm parameters

Algorithm	Parameter	Value
PDR-DCC	$T_3$	1026 $\mu s$
	$T_6$	540 $\mu s$
	$T_9$	370 $\mu s$
	$T_{12}$	290 $\mu s$
	$T_{18}$	200 $\mu s$
	$T_{24}$	170 $\mu s$
LIMERIC	$\alpha$	0.1
	$\beta$	0.033

### 4.3 Implementation of SAE-DCC

#### 4.3.1 WAVE Protocol Stacks

SAE-DCC is implemented on the application layer of the Wireless Access in Vehicular Environment (WAVE) system architecture. For the transport layer and the network layer, IEEE 1609.3 is applied. For the upper layer of MAC, IEEE 1609.4 is introduced for the purpose of multi-channel coordination. The lower layer of MAC and the Physical layer are in accord with IEEE 802.11p. In the physical layer, a 10 MHz channel bandwidth is allocated for the DSRC.

#### 4.3.2 Code Design of SAE-DCC

In our simulation, we have implemented the SAE-DCC in NS3 through C++ programming. For the reason of simplicity, we use (x,y) coordinates instead of (longitude, latitude) to locate each vehicle. Based on the descriptions of SAE-DCC, we have designed the following functions. Meanwhile, the flow chart of the code design is presented in Figure 4.2.

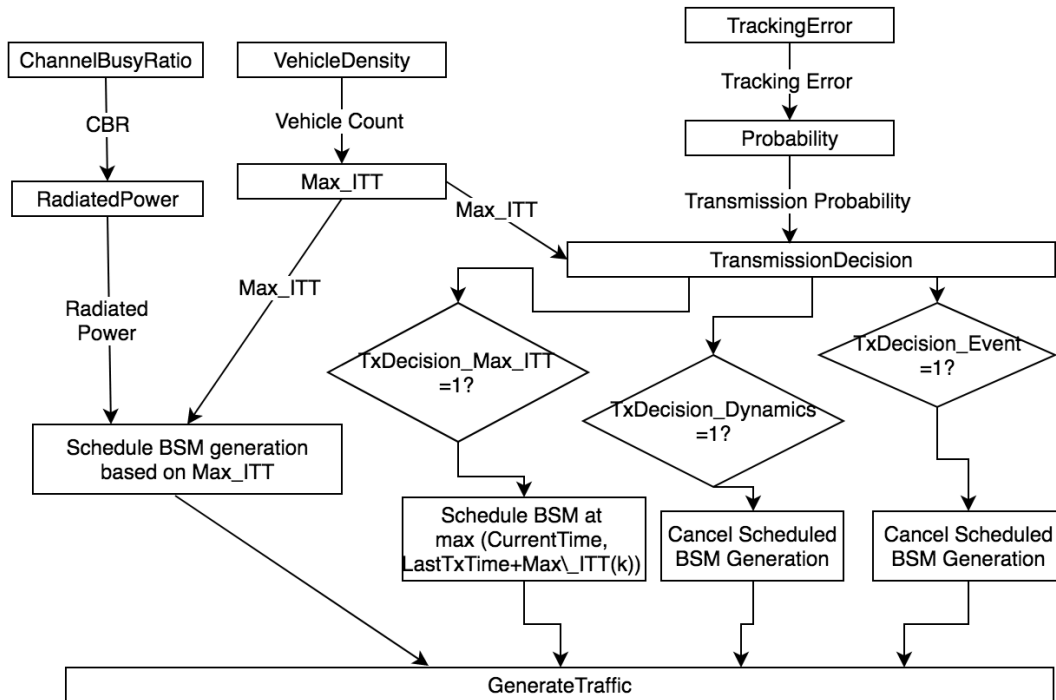


Figure 4.2: SAE-DCC implementation flow chart

**ChannelBusyRatio:** This function is called every 100 ms in order to calculate CBR as shown in Equation 3.1.

**RadiatedPower:** This function is responsible for determining the radiated power w.r.t CBR as shown in Equation 3.6. It is called before the transmission of each BSM packet.

**VehicleDensity:** This function is created for computing the count of unique RVs within 100-meter range. It is called every 1 s.

**Max\_ITT:** This function takes the count of RVs within 100-meter range in order to determine the Max\_ITT as shown in Equation 3.5. It is called every 100 ms.

**ChannelQualityIndicator:** This function is called every 1 s for the calculation of Channel Quality Indicator (CQI) by averaging the PERs of all the RV-HV links during the past 5 s.

**TrackingError:** The intention of this function is to calculate the tracking error. It is called every 100 ms.

**Probability:** With the tracking error as an input, this function determines the transmission probability every 100 ms.

**TransmissionDecision:** This function, called every 100ms or whenever a critical event occurs, is designed to make transmission decisions. If a critical event occurs, TxDecision\_Event is set to 1; if a drawn random number between 0 and 1 is not greater than the transmission probability as well as the time difference between current time and NextScheduledMsgTime is greater than 25 ms, TxDecision\_Dynamics is set to 1; if NextScheduledMsgTime-(LastTxTime+Max\_ITT) is greater than 25 ms, TxDecision\_Max\_ITT is set to 1;

**EventGeneration:** This function is created to simulate the incidence of critical events. It is called randomly and each vehicle will experience one critical event during the 30-second simulation.

**GenerateTraffic:** This function is created for the packet generation. It is called if current time is the NextScheduledMsgTime or TxDecision\_Event is equal to 1 or TxDecision\_Dynamics is equal to 1.



# Chapter 5

## Performance Evaluation

In this chapter, the results of simulations in NS3 will be presented and discussed. Firstly, we will illustrate if SAE-DCC can successfully converge the channel utilization below threshold under three scenarios with various traffic densities. In addition, we will also present the average message rate and the average transmission power for different traffic densities, as SAE-DCC tunes both of these two transmission parameters to obtain the target of congestion control. Secondly, the performance of SAE-DCC, PDR-DCC and LIMERIC will be compared and evaluated using selected evaluation metrics.

### 5.1 Evaluation Metrics

To systematically and extensively evaluate the performance of each DCC algorithm, we selected five metrics: CBR, IRT, position error, T-window reliability and maximum awareness range.

#### 5.1.1 CBR

CBR is the most widely used metric to assess the channel load and it is calculated as the ratio of duration indicated as busy over an observing period. Both energy detection and carrier sensing can contribute to channel busy time, as defined in [19]. According to the research result in [21], it shows that the throughput of successfully delivered packets reaches its peak when the channel utilization is between 0.6 and 0.7. Channel utilization under 0.6 is considered a waste while channel utilization over 0.7 will lead to a high probability of packet collision. Therefore, we set the CBR threshold as 0.7. If the DCC manages to maintain the CBR less than 0.7, it shows the effectiveness of converging the channel load to the target. In our simulation, we synchronize the calculation of CBR for all the vehicles and we will present the average CBR for the vehicles in the observing zone as a function of time for three different traffic densities.

#### 5.1.2 IRT

IRT is the time interval between two successfully delivered packets between a pair of transmitter and receiver. It is calculated at the receiver side based on each communication link. In our result analysis, we sort the calculated IRT values into different distance bins (the step of adjacent distance bins is 25 m) and then we compute the 95<sup>th</sup> percentile IRT for each distance bin (0 m-25 m, 25 m-50 m, 50 m-75 m, etc). The 95<sup>th</sup> percentile IRT is defined as the IRT threshold which is larger than 95% of all measured IRT values.

#### 5.1.3 Position Error

Position error is an application-level metric, which indicates how accurately a RV can track the movement of HV. It is calculated based on each communication link between a pair of transmitter

and receiver.

Whenever a receiver receives a packet from a transmitter, it will interpret the information contained in the packet, including the timestamp, the position, the velocity and the heading angle of the transmitter. Based on the status information, the receiver will extrapolate the transmitter's position using the constant-speed model as shown in Figure 3.2. The position difference in meters between the transmitter's true position and the transmitter's position estimated by the receiver is the position error. In our simulation, we calculate the position error every 0.5 s and the receiver will stop the position tracking if it does not hear from the transmitter for more than 3 s. In terms of the analysis of the position error, we will adopt the same methodology as what we use for the IRT analysis. Firstly, the calculated position error will be sorted into different distance bins (the step of adjacent distance bins is 25 m) and then we will compute the 95<sup>th</sup> percentile position error for each distance bin.

#### 5.1.4 T-window reliability

In order to meet the Requirement of safety applications, at least  $N$  packets are required to be received from its neighbor vehicles in a time window  $T$ . T-window reliability is defined as the probability of successfully receiving at least  $N$  packets from neighbor vehicles during a tolerance time window  $T$  [15]. Each safety application may require different values for  $N$  and  $T$ . For instance, a stationary vehicle warning application requires at least 1 successfully received packet ( $N=1$ ) within a tolerance time window of 1 s ( $T=1$ ) while a lane change warning application requires at least 2 successfully received packets ( $N=2$ ) within a tolerance time window of 1 s ( $T=1$ ) [22]. In our simulation, we analyzed the T-window reliability in different distance bins when  $N$  equals to 1 or 2 while  $T$  remains to be 1.

#### 5.1.5 Maximum Awareness Range

As explained in [23], a communication channel is considered reliable if the probability of satisfying the safety requirements is at least 99%. Thus, we will also calculate and compare the maximum awareness range of each algorithm where its T-window reliability can still be greater than 99%.

## 5.2 Numerical Results Discussion

### 5.2.1 Performance of SAE-DCC

Firstly, we examined the SAE-DCC's ability of converging the channel load below target channel utilization. As illustrated in Figure 5.1, in medium scenario, the average CBR has been well controlled below the 70% threshold and the CBR is quite stable over the simulation period of 30 s. In the dense scenario, the mean value of CBR is slightly greater than the CBR in medium scenario. It shows an overall good ability of converging the channel load, even though there are three time instances when the average CBR values are slightly over the threshold. In terms of the extreme scenario, the average CBR is still below the target CBR, which shows that CBR is able to manage congestion control even under an extremely high vehicular density. In addition, as can be seen in the extreme scenario, SAE-DCC takes approximate 5 s to reach a relatively stable CBR. The reason is that in the simulation we synchronized the introduction of SAE-DCC for all the vehicles and this may lead to some time steps in between. For example, given the fact that most vehicles in the observing zone have similar number of neighboring vehicles within 100-meter range, which leads them to schedule the next packet generation at approximately the same moment, resulting in both extremely busy time intervals and extremely idle time intervals. Gradually, these steps are filled in because of the mobility of the vehicles and finally SAE-DCC is able to maintain a relatively stable CBR.

In these simulations, SAE-DCC has been proved to have a good ability of converging the channel utilization under different traffic densities.

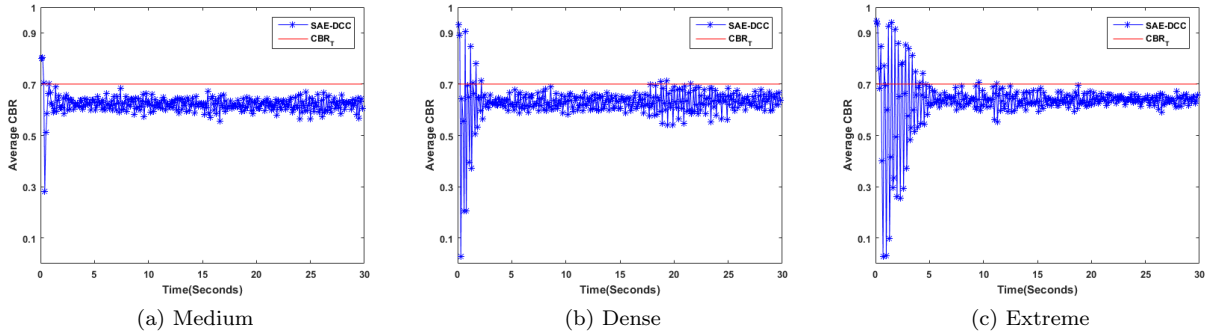


Figure 5.1: CBR in the observing zone of SAE-DCC vs Time for different vehicular densities

Since there is no study showing the selection of the message rate of SAE-DCC under different traffic densities, we also kept tracking the average message rate of SAE-DCC in different simulation scenarios, as presented in Table 5.1. In medium scenario, the message rate of SAE-DCC is 6.28 Hz. If there is no packet generated based on vehicles dynamics or critical events, the message rate can be directly calculated according to Function 3.5, determined exclusively by vehicle counts within 100-meter range. For medium scenario, there are 200 vehicles per kilometer, which leads to 40 vehicles in average within a 100-meter range. Thus, average Max\_ITT is calculated as 160 ms, which signifies that the message rate is 6.25 Hz. Comparing with the message rate we obtained from the simulation (6.28 Hz), it shows that packets generated based on vehicles dynamics or critical events are rare. For the dense and extreme scenarios, the average message rates of SAE-DCC are tuned to 4.08 Hz and 3.18 Hz respectively due to higher traffic densities.

Table 5.1: Average message rate of SAE-DCC in different scenarios

Scenario	Medium	Dense	Extreme
Message Rate	6.28 Hz	4.08 Hz	3.18 Hz

The radiated power is the other transmission parameter tuned by SAE-DCC, which is computed based on CBR, as presented in Equation 3.6. As illustrated in Table 5.2, the average radiated powers obtained from our simulation in different scenarios are 16.915 dBm, 16.685 dBm, and 16.177 dBm.

Table 5.2: Average radiated power of SAE-DCC in different scenarios

Scenario	Medium	Dense	Extreme
Radiated Power	16.915 dBm	16.685 dBm	16.177 dBm

Furthermore, SAE-DCC manages to generate BSM packets according to vehicle dynamics and critical events. For instance, in the medium scenario, at  $t=1.9$  s, the vehicle dynamics condition was met for Vehicle\_206. Thus, the previously scheduled BSM generation at  $t=1.9388$  s was canceled and Vehicle\_206 generated a BSM immediately at  $t=1.9$ s. In view of BSM generation based on critical events, we can notice another instance in the dense scenario. At  $t=16.9148$ s, a critical event occurred to Vehicle\_24, therefore Vehicle\_24 canceled the BSM generation scheduled at  $t=17.035$ s, and generated a BSM with EventFlag immediately.

### 5.2.2 Comparison of CBR

Figure 5.2 presents the CBR of three DCC algorithms under different traffic densities. In addition, Table 5.3 shows the average CBR and the standard deviation after the initial phase. In the medium

scenario, PDR-DCC and SAE-DCC have similar average channel loads at the value of approximate 62%, while the channel load of LIMERIC is roughly 9% lower, which indicates a relatively lower efficiency of channel utilization. In dense scenario, SAE-DCC has the highest average channel utilization (63%) among three DCCs. Compared with medium scenario, the CBR of PDR-DCC in dense scenario drops from 61.70% to 55.42% as PDR-DCC adjusts the data rate from 9 Mbps to 18 Mbps. The CBR of LIMERIC increases from 52.42% to 57.53%. In extreme scenario, compared with the CBR of SAE-DCC (63.84%) and the CBR of LIMERIC (60.02%), the CBR of PDR-DCC (67.11%) is the closest to the target CBR shown as the red line in the figure. In general, all three DCCs show good capabilities of converging the channel loads below the threshold value. However, we can also conclude based on Table 5.3 that PDR-DCC demonstrates the most stable performance in terms of the variation of CBR, while SAE-DCC has the greatest standard variance under three difference traffic densities.

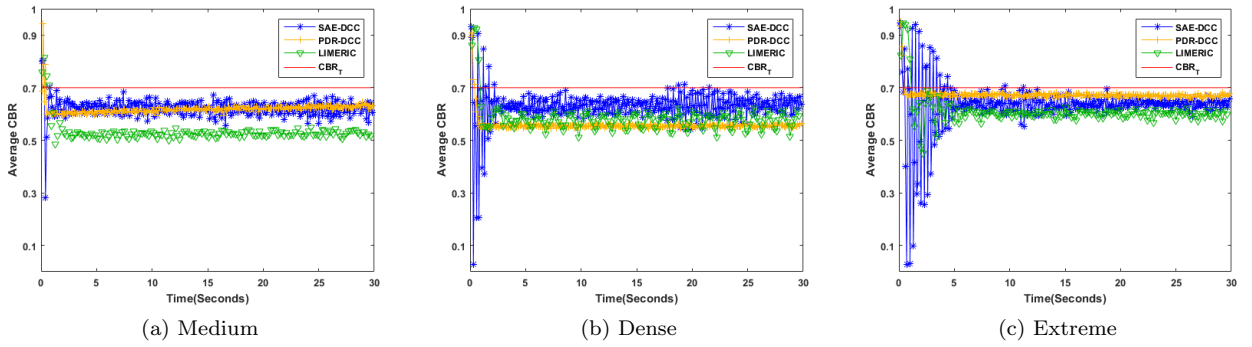


Figure 5.2: CBR vs Time for different vehicular densities

Table 5.3: Average CBR and standard variance in stable phase of three DCCs

DCC Algorithms	Medium		Dense		Extreme	
	Average CBR	Standard Deviation	Average CBR	Standard Deviation	Average CBR	Standard Deviation
SAE-DCC	62.08%	2.18%	63.08%	3.07%	63.84%	2.27%
PDR-DCC	61.70%	0.97%	55.42%	0.41%	67.11%	0.50%
LIMERIC	52.42%	1.01%	57.53%	2.68%	60.02%	1.25%

### 5.2.3 Comparison of IRT

The results of 95% IRT of DCCs sorted into different distance bins are presented in Figure 5.3 (medium), Figure 5.4 (dense) and Figure 5.5 (extreme). For each traffic density, we present two subfigures, one on the left side illustrating the 95% IRT from 0 m to 450 m while the other one on the right side focusing on the range from 0 m to 200 m, as neighbor vehicles within 200 m are more crucial than those beyond 200 m due to a shorter tolerance in the reaction time.

In medium scenario, as shown in Figure 5.3, in near area (within 200 m), the 95% IRT of PDR-DCC noticeably outweighs the other two DCCs given the fact that its message rate (10 Hz) is the highest. However, from 175 m onwards, the IRT difference between PDR-DCC and the other two DCCs tends to get smaller. Because the data rate of PDR-DCC in medium scenario is tuned to 9 Mbps while the data rates of LIMERIC and SAE-DCC are 6 Mbps, PDR-DCC has a worse robustness against the interference and noise. When the distance gets longer, the packet delivery ratio of PDR-DCC will decrease, resulting in a shorter communication range. LIMERIC and SAE-DCC have similar IRT performance within the range of 200 m, as their message rates are very close (the average message rates of SAE-DCC and LIMERIC are 6.28 Hz and 5.95 Hz

respectively). But for the longer distance, LIMERIC has a slightly smaller IRT than SAE-DCC. In view of the above discussion, PDR-DCC demonstrates the best IRT performance in medium scenario for both longer and shorter distances.

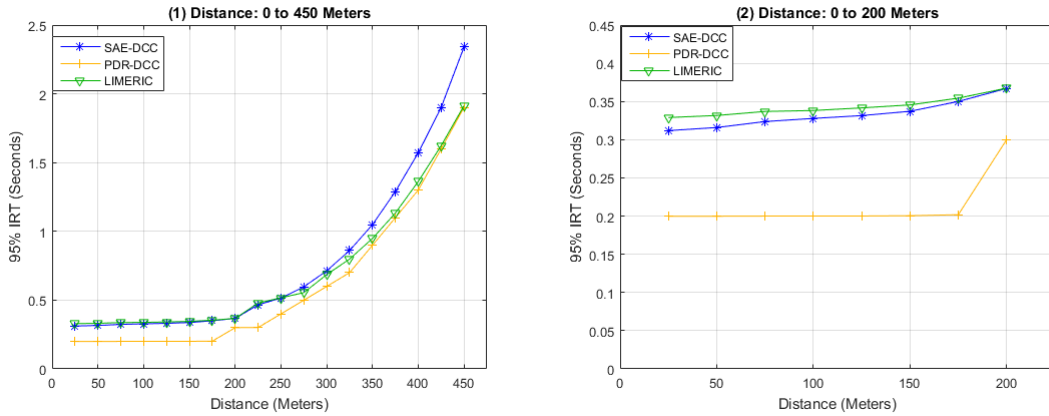


Figure 5.3: 95% IRT vs distance in medium scenario

In dense scenario as shown in Figure 5.4, similar to the IRT results in medium scenario, in the near area PDR-DCC predominates among all the DCCs due to its high message rate of 10 Hz. However, IRT of PDR-DCC starts to increase rapidly from 175 m and PDR-DCC shows the worst IRT performance compared with the other two DCCs from 325 m onwards. This is because the data rate of PDR-DCC is tuned from 9 Mbps to 18 Mbps for reaching the goal of congestion control. As explained before, a higher data-rate always leads to a worse robustness against the noise and interference, hence the communication range of PDR-DCC in dense scenario becomes even shorter compared with the medium scenario. LIMERIC and SAE-DCC still have similar IRT performance within the range of 200 m, as their message rates are very close (the average message rates of SAE-DCC and LIMERIC are 4.08 Hz and 4.37 Hz respectively). But for longer distance, LIMERIC demonstrates a better IRT performance than SAE-DCC. To sum up, in dense scenario, PDR-DCC has the best IRT performance for shorter distance while LIMERIC excels the other two DCCs for longer distance.

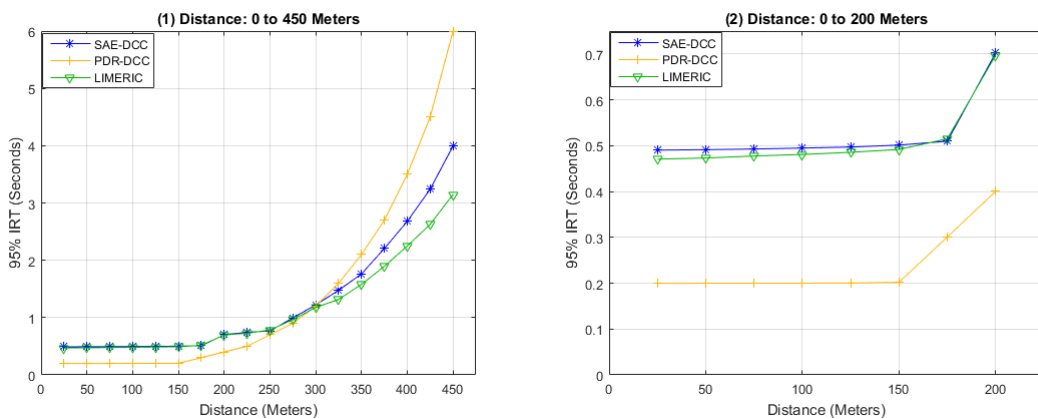


Figure 5.4: 95% IRT vs distance in dense scenario

In extreme scenario, as shown in Figure 5.5, the result is roughly in accordance with the result in dense scenario. PDR-DCC leads in the IRT performance for shorter distance while LIMERIC is the best for longer distance. One more noticeable result is that the gap between IRT of PDR-DCC and the other two DCCs in extreme scenario is wider than the gap in dense scenario. This

is because a fixed message rate of 10 Hz in extreme scenario will lead to a higher probability of packet collision.

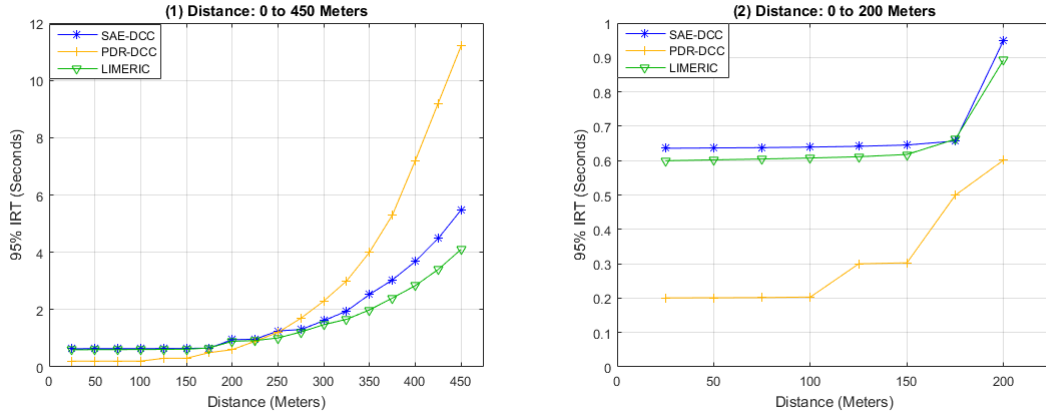


Figure 5.5: 95% IRT vs distance in extreme scenario

### 5.2.4 Comparison of Position Error

The 95% position error sorted into different distance bins are presented in Figure 5.6 (medium), Figure 5.7 (dense) and Figure 5.8 (extreme). For each traffic density, we present two subfigures, one on the left side illustrating the 95% position error from 0 m to 500 m while the other one on the right side focusing on the range within 200 m which is a more critical region.

In medium scenario, as shown in Figure 5.6, within 200 m, the position error of PDR-DCC is the smallest due to its shortest IRT as shown in Figure 5.3, while the position error of SAE-DCC and LIMERIC are greater. However, when the distance becomes longer, the position error of PDR-DCC grows rapidly and all three algorithms tend to have similar position error performances while the position error of SAE-DCC is slightly larger than the other two DCCs.

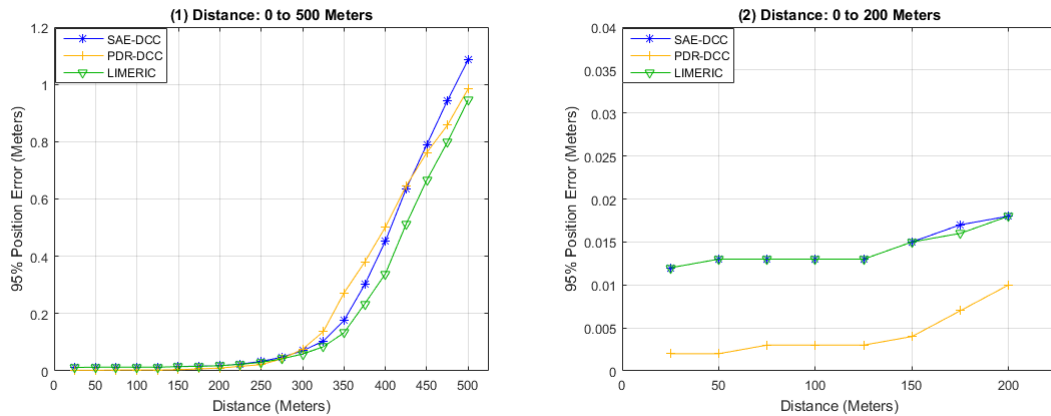


Figure 5.6: 95% position error vs distance in medium scenario

For both dense and extreme scenarios, as shown in Figure 5.7 and Figure 5.8, PDR-DCC outweighs the other two algorithms in near region while LIMERIC demonstrates the best position error performance for the longer distance. This result is consistent with the IRT performance, since the determining factor of position error is the packet inter-reception time.

If we compare the position error vertically, we found that when the vehicular density increases from 200 vehicles per kilometer to 400 vehicles per kilometer, the position error actually decreases.

This is because vehicles are forced to have a smaller maximum velocity and a smaller maximum acceleration under a high traffic density, which leads to a smaller oscillation of position error.

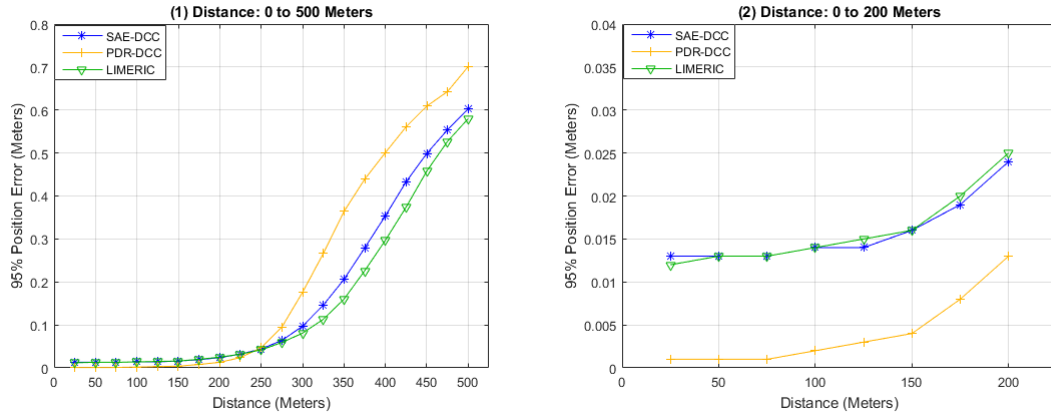


Figure 5.7: 95% position error vs distance in dense scenario

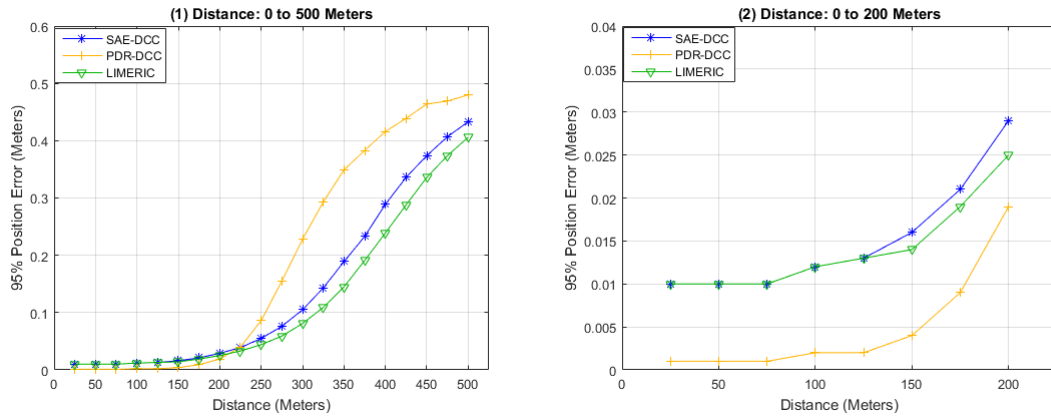


Figure 5.8: 95% position error vs distance in extreme scenario

### 5.2.5 Comparison of T-window Reliability

In terms of T-window reliability, we analyzed the communication requirements for two safety applications, the stationary vehicle warning application ( $N=1$ ,  $T=1$ ) and the lane change warning application ( $N=2$ ,  $T=1$ ).

Figure 5.9 presents the T-window reliability of the stationary vehicle warning application ( $N=1$ ,  $T=1$ ) under different vehicular densities. In medium scenario, as shown in Figure 5.9 (a), within the range of 225 m, all three DCCs have similar T-window reliability. However when the distance becomes longer, T-window reliability of PDR-DCC tends to be left behind by LIMERIC and SAE-DCC while LIMERIC takes the lead. In dense scenario, as shown in Figure 5.9 (b), the T-window reliability of PDR-DCC moderately prevails within the range of 225 m. For longer distance, the T-window reliability of PDR-DCC drops remarkably and SAE-DCC starts to take the lead. In extreme scenario, as shown in Figure 5.9 (c), the T-window reliability of PDR-DCC drops even more drastically when the distance gets longer. However, PDR-DCC still demonstrates the best performance of T-window reliability in the near region.

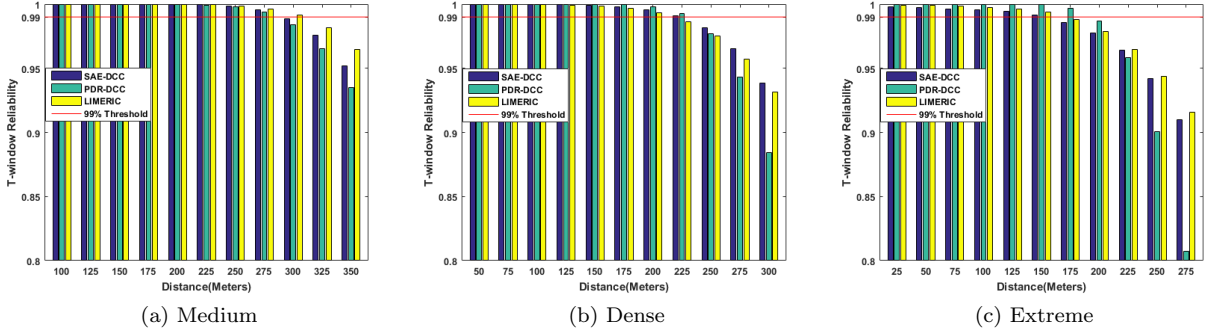
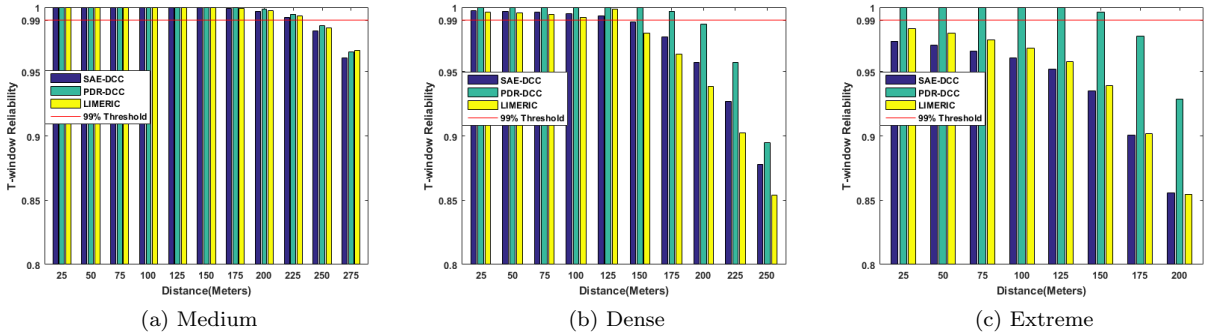

 Figure 5.9: T-window reliability ( $N=1$ ,  $T=1$ ) under different traffic densities

Figure 5.10 presents the T-window reliability of the lane change warning application ( $N=2$ ,  $T=1$ ) under different vehicular densities. For all the scenarios with various traffic densities, PDR-DCC shows the best T-window reliability performance compared with LIMERIC and SAE-DCC. Because PDR-DCC transmits packets at a fixed message rate of 10 Hz, it has a higher possibility to guarantee at least two packets received within 1 s. However both LIMERIC and SAE-DCC adjust the message rate to converge the channel loads. In extreme scenario particularly, the message rates of LIMERIC and SAE-DCC are adjusted to very low values (3.56 Hz and 3.18 Hz respectively), which degrades the T-window reliability when at least two packets are required to be received within 1 s.


 Figure 5.10: T-window reliability ( $N=2$ ,  $T=1$ ) under different traffic densities

## 5.2.6 Comparison of Maximum Awareness Range

The red horizontal lines in Figure 5.9 and Figure 5.10 indicate the 99% T-window reliability, according to which we obtained the maximum awareness range for each DCC under different vehicular densities, as listed in Table 5.4.

Firstly, we focus on the performances of DCCs when the safety application requires only 1 received packet within 1 s. In medium scenario, LIMERIC has the longest maximum awareness range as 300 m, which is 25 m longer than the other two algorithms. In dense scenario, PDR-DCC and SAE-DCC have the same maximum awareness range while the value of LIMERIC is 25 m shorter. However, in extreme scenario, PDR-DCC starts to show its strength since the message rates of LIMERIC and SAE-DCC are significantly lowered.

According to the maximum awareness range result when at least 2 packets are required to be received within 1 s, PDR-DCC shows a clear advantage under high traffic densities. In medium scenario, all three DCCs manage to obtain an awareness range of 225 m. In dense scenario, the



awareness range of PDR-DCC is already 50 m longer than the other two DDCs. In extreme scenario, the awareness ranges of LIMERIC and SAE-DCC drop to 0 while PDR-DCC is still able to maintain a 150-meter value.

Table 5.4: Maximum awareness range for different application requirements under various traffic densities

Application requirement	Density	Maximum awareness range(meters)		
		SAE-DCC	PDR-DCC	LIMERIC
N=1, T=1 sec	Medium	275	275	<b>300</b>
	Dense	<b>225</b>	<b>225</b>	200
	Extreme	150	<b>175</b>	150
N=2, T=1 sec	Medium	<b>225</b>	<b>225</b>	<b>225</b>
	Dense	125	<b>175</b>	125
	Extreme	0	<b>150</b>	0

### 5.2.7 Impact of CCA Busy Threshold on SAE-DCC

In addition to the comparison with other DCCs, we also conducted an extra simulation to understand the impact of CCA Busy Threshold on SAE-DCC. As introduced before, the US standard defines the received power sensitivity as -92 dBm and the CCA busy threshold as -95 dBm while the European standard specifies these two values as -82 dBm and -85 dBm respectively. In practice, this improves the requirements for sensor manufacturers, therefore we apply the European parameters to the SAE-DCC in medium scenario to see if increasing the CCA busy threshold will degrade the performance of SAE-DCC.

As shown in Figure 5.11, increasing the CCA busy threshold from -95 dBm to -85 dBm actually makes the CBR lower ( from 62% to 48%). This is because a higher CCA busy threshold will shorten the transmission range. However, the message rate does not change, because it is determined by the number of neighbor vehicles within the 100-meter range as presented in Equation 3.5. Thus, we can conclude that in medium scenario SAE-DCC does not efficiently use the communication channel when the CCA busy threshold increases to -85 dBm.

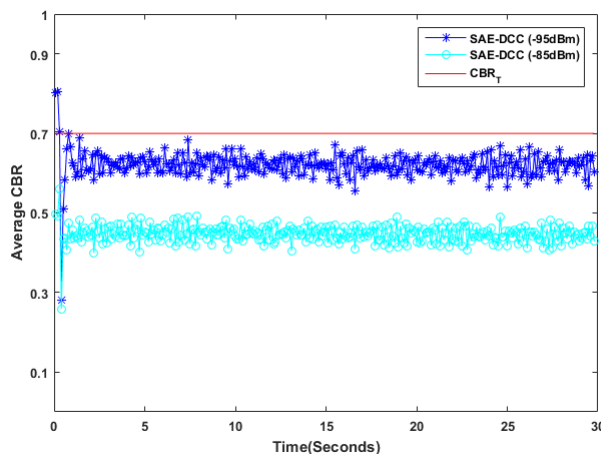


Figure 5.11: CBR comparison of SAE-DCC with different CCA busy thresholds in medium scenario

Figure 5.12 and Figure 5.13 present the IRT and the position error comparison respectively. As we can see from the figures, within 150-meter range, SAE-DCC with CCA busy threshold as

-85 dBm shows a better performance. However, as the distance increases, SAE-DCC with CCA busy threshold as -95 dBm starts to prevail due to a longer communication range.

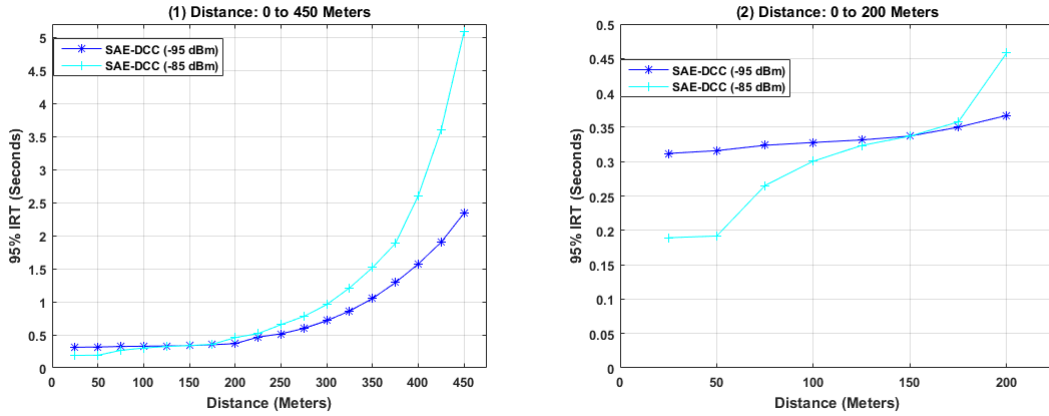


Figure 5.12: 95% IRT comparison of SAE-DCC with different CCA busy thresholds in medium scenario

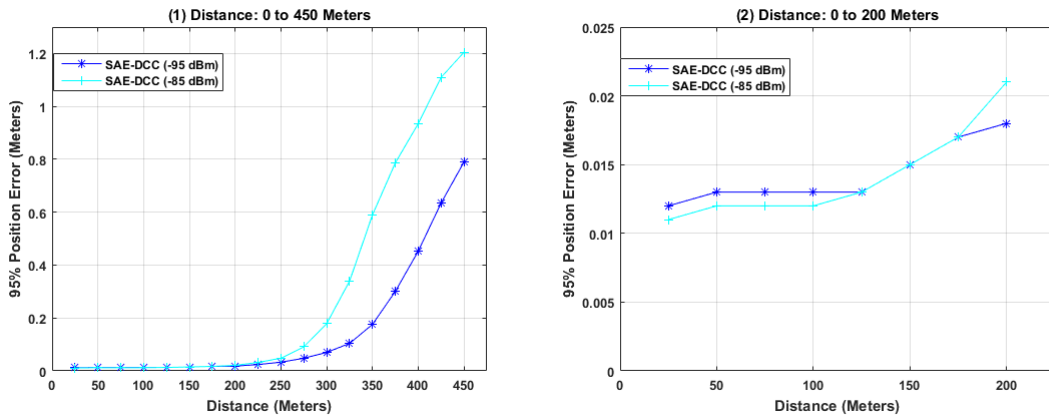


Figure 5.13: 95% Position error comparison of SAE-DCC with different CCA busy thresholds in medium scenario

As presented in Figure 5.14, the CCA threshold of -95 dBm provides a better performance of T-window reliability ( $N=1$ ,  $T=1$ ) in medium scenario. As the distance increases, it shows a greater advantage. The reason is that increasing the CCA threshold shortens the communication range. Thus, it will have a worse performance for transmitter-receiver links with long distances.

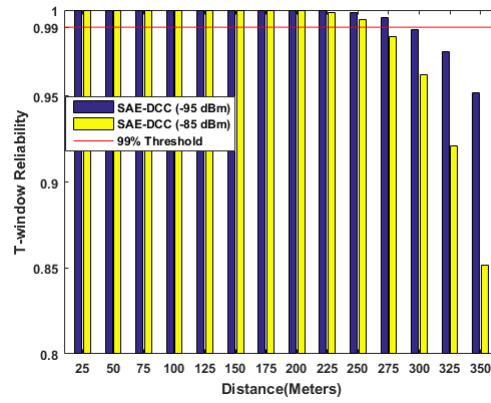


Figure 5.14: T-window reliability (N=1, T=1) comparison of SAE-DCC with different CCA busy thresholds in medium density scenario

## Chapter 6

# Conclusion and Future Work

### 6.1 Conclusions

In this thesis, we investigated the effectiveness of SAE-DCC and also compared its performance with two selected DCC algorithms.

According to our simulation results in NS3 simulator, SAE-DCC shows a good capability of controlling the channel utilization even if the vehicular density reaches 400 vehicles/km. Thus, our study verifies that SAE-DCC is capable of congestion control under different vehicular densities.

Having proved the effectiveness of SAE-DCC, we also benchmarked its performance with PDR-DCC and LIMERIC. Based on the CBR performance, we concluded that PDR-DCC is the most stable after the transition phase while SAE-DCC is the most sensitive to the vehicular mobility as it has the greatest variance. In terms of IRT and position error performances, SAE-DCC and LIMERIC show very similar results as their derived message transmission rates are similar as well. For vehicles within 200-meter range, PDR-DCC provides a shorter IRT and a smaller position error, which indicates that PDR-DCC can provide a better freshness of received packets and a more accurate tracking of transmitter's position. But for vehicles beyond 200 m, SAE-DCC and LIMERIC tend to outweigh PDR-DCC. This is because a higher data-rate message has a shorter communication range. From the perspective of T-window reliability and the maximum awareness range, PDR-DCC overall outperforms the other two DCCs due to its fixed message rate of 10 Hz, especially for high density scenarios and for safety applications requiring more than 1 received packet per 1 second. In view of the impact of CCA busy threshold on SAE-DCC via simulations of the medium density scenario, the values specified in US standard is more suitable for SAE-DCC.

### 6.2 Future Work

Several research studies can be conducted in the future for extending the understanding of SAE-DCC.

1. We have evaluated the performance of SAE-DCC in the highway scenarios with straight lanes. However, the performance of SAE-DCC in other road situations, e.g curved roads remains unknown. Given the fact that a curved road will lead to a higher vehicle dynamics, SAE-DCC will generate and transmit more packets based on vehicle dynamics. This might increase its message rate and will have an impact on its communication-level and application-level reliability. Thus, some new simulations in curved roads need to be conducted for this purpose.
2. In our study, we analyzed the performance of SAE-DCC in medium scenario if we change the CCA threshold from the value specified in the US standard to the value specified in the European standard. More simulations need conducting in order to see the performance of SAE-DCC in dense and extreme scenario after changing the CCA threshold.

3. SAE-DCC adjusts the message rate and the radiated power to converge the channel loads while data rate remains at 6 Mbps. Further studies need to be conducted to see how SAE-DCC in combination with adjusting data rate can improve its performance.

# Bibliography

- [1] A. Donnelly, “The annual cost of u.s. traffic congestion.” Available at <https://www.mikogo.com/2015/09/30/us-traffic-congestion/> (2017/07/26). 1
- [2] F. C. Commission, “Notice of Proposed Rulemaking and Order FCC 03-324,” Feb.2003. 1
- [3] “Intelligent Transport Systems (ITS); Vehicular Communications; Basic Set of Applications; Part 3: Specifications of Decentralized Environmental Notification Basic Service,” Technical Report, ETSI TS 102 637-3 V1.1.1, 2010. 2
- [4] “Dedicated Short Range Communications (DSRC) Message Set Dictionary,” Technical Report, SAE International, J2735<sup>TM</sup>, 2010. 2, 9
- [5] C. B. Math, A. Ozgur, S. H. de Groot, and H. Li, “Data rate based congestion control in v2v communication for traffic safety applications,” in *Communications and Vehicular Technology in the Benelux (SCVT), 2015 IEEE Symposium on*, pp. 1–6, IEEE, 2015. 2, 4
- [6] G. Bansal, J. B. Kenney, and C. E. Rohrs, “Limeric: A linear adaptive message rate algorithm for dsrc congestion control,” *IEEE Transactions on Vehicular Technology*, vol. 62, no. 9, pp. 4182–4197, 2013. 2, 4, 5, 13
- [7] C. B. Math, H. Li, S. H. de Groot, and I. Niemegeers, “Fair decentralized data-rate congestion control for v2v communications,” in *24th International Conference on Telecommunications*, IEEE, 2017. 2, 4, 5, 13
- [8] “On-Board System Requirements for V2V Safety Communications,” Technical Report, SAE International, J2945<sup>TM</sup>, Mar. 2016. 2, 10, 13
- [9] “Vehicle Safety Communications Project Task 3 Final Report: Identify Intelligent Vehicle Safety Applications Enabled by DSRC,” *The CAMP Vehicle Safety Communications Consortium*, 2005. 3
- [10] T. Tielert, D. Jiang, Q. Chen, L. Delgrossi, and H. Hartenstein, “Design methodology and evaluation of rate adaptation based congestion control for vehicle safety communications,” in *Vehicular Networking Conference (VNC), 2011 IEEE*, pp. 116–123, IEEE, 2011. 4
- [11] G. Bansal, H. Lu, J. B. Kenney, and C. Poellabauer, “Embarc: Error model based adaptive rate control for vehicle-to-vehicle communications,” in *Proceeding of the tenth ACM international workshop on Vehicular inter-networking, systems, and applications*, pp. 41–50, ACM, 2013. 4
- [12] G. Caizzone, P. Giacomazzi, L. Musumeci, and G. Verticale, “A power control algorithm with high channel availability for vehicular ad hoc networks,” in *Communications, 2005. ICC 2005. 2005 IEEE International Conference on*, vol. 5, pp. 3171–3176, IEEE, 2005. 4
- [13] J. Maurer, T. Fugen, and W. Wiesbeck, “Physical layer simulations of ieee802. 11a for vehicle-to-vehicle communications,” in *Vehicular Technology Conference, 2005. VTC-2005-Fall. 2005 IEEE 62nd*, vol. 3, pp. 1849–1853, IEEE, 2005. 4

- [14] T. Tielert, D. Jiang, H. Hartenstein, and L. Delgrossi, "Joint power/rate congestion control optimizing packet reception in vehicle safety communications," in *Proceeding of the tenth ACM international workshop on Vehicular inter-networking, systems, and applications*, pp. 51–60, ACM, 2013. 4
- [15] F. Bai and H. Krishnan, "Reliability analysis of dsrc wireless communication for vehicle safety applications," in *Intelligent Transportation Systems Conference, 2006. ITSC'06. IEEE*, pp. 355–362, IEEE, 2006. 6, 17
- [16] T. ElBatt, S. K. Goel, G. Holland, H. Krishnan, and J. Parikh, "Cooperative collision warning using dedicated short range wireless communications," in *Proceedings of the 3rd international workshop on Vehicular ad hoc networks*, pp. 1–9, ACM, 2006. 6
- [17] C. B. Math, H. Li, and S. H. de Groot, "Risk assessment for traffic safety applications with v2v communications," in *Vehicular Technology Conference (VTC-Fall), 2016 IEEE 84th*, pp. 1–6, IEEE, 2016. 6
- [18] G. Bansal, B. Cheng, A. Rostami, K. Sjoberg, J. B. Kenney, and M. Gruteser, "Comparing limeric and dcc approaches for vanet channel congestion control," in *Wireless Vehicular Communications (WiVeC), 2014 IEEE 6th International Symposium on*, pp. 1–7, IEEE, 2014. 6
- [19] "Standard for LAN/MAN - Specific requirements Part 11: Wireless LAN Medium Access Control (MAC) and Physical Layer (PHY) Specifications," *IEEE Std. 802.11<sup>TM</sup>*, 2012. 7, 16
- [20] "Intelligent Transport Systems (ITS); STDMA recommended parameters and settings for cooperative ITS; Access Layer Part," Technical Report, ETSI TR 102 861 V1.1.1, Jan. 2012. 13
- [21] Y. P. Fallah, C.-L. Huang, R. Sengupta, and H. Krishnan, "Analysis of information dissemination in vehicular ad-hoc networks with application to cooperative vehicle safety systems," in *IEEE Transactions on Vehicular Technology*, pp. 233–247, IEEE, 2011. 16
- [22] C. B. Math, H. Li, S. H. de Groot, and I. Niemegeers, "V2x application-reliability analysis of data-rate and message-rate congestion control algorithms," *IEEE Communications Letters*, 2017. 17
- [23] N. An, T. Gaugel, and H. Hartenstein, "Vanet: Is 95% probability of packet reception safe?," in *ITS Telecommunications (ITST), 2011 11th International Conference on*, pp. 113–119, IEEE, 2011. 17